Research and Reviews Journal of Microbiology and Biotechnology

e-ISSN: 2320-3528
p-ISSN: 2347-2286

Activation of Autophagy Through the NLRP3/mTOR Pathway: A Potential Mechanism for Alleviation of Pneumonia by QingFei Yin Recipe

Xiaozhou Sun[1]*, Dandan Wang[1], Lizhong Ding[4] ,Yan Xu[1], Wenxiu Qi[3], Daqing Zhao[3] ,Li Liu[1], Cheng cheng Yin[1], Changsheng Cui[1], Zhongtian Wang[1], Liwei Sun[2]*,LipingSun[4]*

[1]Research Center of Traditional Chinese Medicine, Changchun University of Chinese Medicine, Changchun, Jilin, China

[2] Research Center of Traditional Chinese Medicine, The Affiliated Hospital to Changchun University of Chinese Medicine, Changchun, Jilin, China

[3] Jilin Provincial Key Laboratory of Bio Macromolecules of Chinese Medicine, Jilin Ginseng Academy, Changchun University of Chinese Medicine, Changchun, Jilin, China

[4] Center of Children's Clinic, The Affiliated Hospital to Changchun University of Chinese Medicine, Changchun, Jilin, China

Research Article

Received date: 10/02/2021
Accepted date: 24/02/2021
Published date: 03/03/2021

***For Correspondence**
Liwei Sun, Liping Sun, Research Center of Traditional Chinese Medicine, The Affiliated Hospital to Changchun University of Chinese Medicine, Changchun, Jilin, China

E-mail: sunnylilwei@163.com

Keywords: *Proteomics, Streptococcus pneumonia,*

ABSTRACT

Qing-Fei Yin(QFY), a Chinese traditional medicine recipe, is known for its excellent therapeutic efficacy for the treatment of bacterial lung infections, although its molecular mechanism of action remains unknown. Here, QFY chemical composition was determined using the High Performance Liquid Chromatography-Mass(HPLC-MS/MS) method, and then QFY was evaluated for protective efficacy against pneumonia using two models: a *Streptococcus pneumoniae*-induced *in vivo* mouse model and an *in vitro* Pneumolysin (PLY)-induced murine lung alveolar-derived MH-S cell line-based model. Notably, QFY exerted prominent anti-pneumonia effects both *in vivo* and *in vitro*. To further explore QFY protective effects, 4D Label free proteomics analysis, pathologic evaluation and Immunohistochemical (IHC) analysis were conducted to identify pathways involved in QFY protection. Notably, pivotal

e-ISSN: 2320-3528
p-ISSN: 2347-2286

Pneumonia,NLRP3 Inflammasome, Autophagy, QingFei Yin recipe

roles for NLRP3 inflammasome and autophagy pathways were found to be pharmacologically important for QFY-based protection, with both pathways shown to reciprocally regulate one another. Briefly, QFY triggered autophagy via down-regulation of upstream NLRP3/mTOR signalling pathway events, resulting in quenching of the NF-κB pathway and amelioration of inflammatory injury. Collectively, our results reveal molecular mechanisms underlying QFY protection against pneumonia as a foundation for the future development of novel treatment therapy to combat this disease and reduce antibiotic abuse.

INTRODUCTION

Pneumonia, a type of acute lower respiratory infection, accounts for an extremely large proportion of the overall worldwide disease burden[1-3]. *Streptococcus pneumoniae*(*S.pn*), a gram-positive bacterium, is recognized as the most common cause of pathogen-induced pneumonia, while also causing respiratory tract infections, pulmonary parenchymal inflammation and pulmonary infection-derived bacteremia[2,3]. Such dire pathological effects have been shown to involve the Pneumococcal Cytolysin Pneumolysin(PLY), a major virulence factor expressed by almost all pneumonia-causing *S.pn* bacteria[4, 5]. Importantly, PLY toxin possesses a unique feature whereby it can induce host pore-dependent pro-inflammatory responses[5] that appear to play major roles in pneumococcal pathogenicity. The advent of antibiotic use has greatly diminished pneumonia mortality rates. However, the emergence and spread of antibiotic resistance worldwide has directly resulted in the need for physicians to prolong administration of pneumonia treatments, leading to increased incidence of complications and greater mortality[6-9]. Therefore, treatment strategies for pneumonia must be administered with extraordinary care by the biomedical community[11]. Meanwhile, Traditional Chinese Medicines(TCM) as alternative treatments have been attracting increasing attention around the world, due to their long history of clinical use and proven therapeutic efficacy for alleviating infectious diseases[11-16]. Qing Fei Yin (QFY), a Chinese traditional medicine recipe(containing Belamcandae Rhizoma, Forsythia, Fritillaria Cirrhosa and Scutellaria baicalensis) evolved from the Gan Lu Xiao Du pill in the Chinese classic “Yi Xiao Mi Chuan”,has been widely used for clinical treatment of pneumonia. The excellent therapeutic effect suggests the potential of QFY in reducing the use of antibiotics, although the molecular mechanism underlying QFY alleviation of pneumonia remains unclear. High-throughput proteomics tools have been widely recognized as useful for exploring the pharmacology of complex TCM systems[17-19]. Therefore, in this study the *in vivo* curative effect of QFY was evaluated in *S.pn*-infected mice, with changes in protein expression before and after QFY treatment systematically compared using a method based on application of 4D Label free proteomics analysis. Our results identified 655 and 345 differentially expressed proteins based on comparisons between their levels in the control group versus *S.pn* group and between the *S.pn*+QFY group versus *S.pn* group, respectively. Subsequently, Geneontology (GO) and Kyoto Encyclopedia of Genes and Genomes (KEGG) pathway analysis strongly implicated involvement of more than 40 differentially expressed proteins associated with NOD-like receptor-dependent and autophagy pathway-dependent functions. These results prompted us to surmise that NLRP3 and autophagy were both associated with development of *S.pn*-induced infectious disease and highlight their potential value as targets

e-ISSN: 2320-3528
p-ISSN: 2347-2286

of QFY-based therapy. It has become evident that the host inflammatory reaction to a pathogen can play a predominant role in infectious disease outcomes. Recent studies have suggested that
macrophage surface and Intracellular Toll-like (TLRs) and Nucleotide-binding Oligomerization Domain (NOD) like receptors (NLRs) may participate in pathogen sensing and inflammatory responses[20-21]. Unlike TLRs, which directly recognize their agonists, NLRs are associated with inflammasome activation and caspase-1 (cysteinyl aspartate-specific proteinase-1)-dependent pro-IL-1β/IL-18 release. NLRP3 (NOD-like receptor protein 3), a well-known member of the NLRs family, binds to its adaptor protein Apoptosis-associated Speck-like protein (ASC) containing a C-terminal Caspase Recruitment Domain (CARD)). This binding event leads to the recruitment of pro-caspase-1 which results in formation of a multiprotein complex, the NLRP3 inflammasome[20-22]. Meanwhile, mounting evidence has revealed a bidirectional modulatory effect of NLRP3 on bacterial invasive disease. More specifically, during the initial period of *S.pn* invasion, NLRP3 contributes to protective immunity and host defense[23-25]. However, during late-stage infection, PLY-activated NLRP3 inflammasomes trigger alveolar epithelial cells and macrophages to over-release mature inflammatory cytokines that subsequently enhance the inflammatory response and ultimately promote progression to pneumoni[26-29]. Aside from inflammasome based host defenses, autophagy has recently attracted attention as a critically important homeostatic process involved in host defenses and multicellular immunity. Importantly, autophagy acts to reduce bacterial burden and microbial tissue damage by eliminating invading pathogens[30]. Consequently, promotion of autophagy to inhibit inflammasomes activation may be an effective therapeutic approach for prevention and treatment of *S.pn*-induced pneumonia. Nevertheless, it is important to note that NLRP3 and autophagy are linked by reciprocal regulatory processes[31-33]. For example, it appears that degradation of NLRP3 inflammasomes partly depends on autophagy[34]. Indeed accumulating evidence suggests that such processes may function within a bidirectional regulatory network linking NLRP3 to autophagy[35,36].Meanwhile, NLRP3 has been identified as a binding partner of mTOR, whereby NLRP3 mechanistically inhibits autophagy by promoting mTOR phosphorylation. In turn, autophagy is an essential process for governing NLRP3 activation[33]. Therefore, NLRP3 and autophagy have become newly recognized potential treatment targets for use in combating *S.pn*-based infectious diseases. However, complex bidirectional regulatory mechanisms operating within the NLRP3-autophagy axis and the precise target of QFY action remain unclear and were therefore selected for comprehensive investigation in this work.

MATERIALS AND METHODS

Materials and reagents

S. pneumoniae serotype 2 strain D39, a type 2 pneumococcal strain, was provided by Zunyi Medical College. Culture medium components were purchased from commercial vendors as follows: PLY from Fitzgerald(Acton, MA, USA), Todd Hewitt broth from Difco (Detroit, MI, USA),RPMI 1640 medium from Gibco (New York, NY, USA),and fetal bovine serum(FBS)from CLARK Bioscience(Claymont, DE, USA).The MH-S cell line was purchased from the Cell Bank of the Chinese Academy of Sciences and derived from alveolar macrophages of 7-week-old mice (Shang Hai, China). Mouse interleukin-lβ(IL-1β, #MLB00C),tumor necrosis factor-alpha(TNF-α, #MTA00B),and interleukin-6(IL-6, #M6000B) Enzyme-Linked Immunosorbent Assay (ELISA) kits were obtained commercially (R&D Systems, Minneapolis,MN,USA).Rabbit polyclonal antibodies against ULK(#ab167139),p62(#ab155686),NF-κB P65

e-ISSN: 2320-3528
p-ISSN: 2347-2286

(#ab16502),NF-κB p-P65(#ab194726),IκB(#ab7217)LC3B(#ab51520), and β-tubulin(#ab18207) were purchased from Abcam(Cambridge, MA, USA).Rabbit monoclonal antibodies against mTOR(#ab32028), p-mTOR (#ab109268), and p-ULK(#ab229909) and mouse monoclonal antibodies against GAPDH(#ab8245) were purchased from Abcam. Rabbit polyclonal antibodies against NLRP3(#15101S),ASC(#67824T),and cleaved casp1(#89332S) were purchased from Cell Signaling Technology (Beverly, MA, USA).3-Methyladenine,a PI3K inhibitor and inhibitor of autophagy(3-MA, #HY-19312),and MCC950 sodium(#HY-12815A),an inhibitor of NLRP3,were purchased from MCE(Beverly, MA, USA).

Preparation of QFY and components identification

QFY was provided by the Affiliated Hospital of Changchun University of Traditional Chinese Medicine (Jilin, China). Each component powder was accurately weighed and formulated to generate QFY according to the following ratio(by weight- Belamcandae Rhizoma, Forsythia, Fritillaria Cirrhosa and Scutellaria baicalensis of 0.4:0.4:0.05:0.15.The compounds in the recipe were identified with LC-MS/MS conditions as follows:
Chromatographic(Thermo, Ultimate 3000LC,Q Exactive HF)separations were accomplished on a Zorbax Eclipse C18(1.8 μm*2.1*100 mm).The mobile phase consisted of 0.1% formic acid water(phase A)and acetonitrile (phase B) at 0.3 ml/min with 1:1 splitter ratio and a gradient elution. The gradient change of acetonitrile(B)was 0-2 min, 5% B; 2-6 min, 30%B; 6-7 min, 30%B; 7-12 min,78%B; 12-14 min,78%B;14-17 min, 95%B;17-20 min,95%B; 20-21 min, 5%B;21-25 min, 5%B. 2 μL of sample was injected at room temperature. The mass spectrometer was operated both in the positive and negative ion modes. The following instrument parameters were applied:heater temperature of 325°C, ion spray voltage of 3.5 kV, sheath gas flow velocity of 45 arb, auxiliary gas velocity of 15 arb, scavenging air velocity of 1 arb, S-Lens RF Level of 55%. Scanning mode:full scan(m/z 100~1500)and Data dependent second-order mass spectrometry scanning(dd-MS2,TopN=10); Collision mode:High Energy collision Dissociation(HCD).The mixture was placed in a conical flask then it was mixed with 10 ml 70% ethanol. After placing a cork in the flask, the mixture was shocked for 40 min (power 250 W, frequency 50 kHz).After shocking, the mixture was centrifuged at 4000 rpm/min for 15 min to yield a supernatant containing QFY that was then filtered(0.22 μm).Ten batches of QFY compound from different sources were each separated using a ZORBAX Eclipse Plus C18(4.6 mm×250 mm,5-μm) HPLC system(Shimadzu,Kyoto,Japan) and a diode array detector(UltiMate 3000,DIONEX,Sunnyvale,CA,USA).Analysis of specific components in each batch yielded chemical fingerprints (supplemental Table 1)[37-39]. The mobile phase condition was recorded as follows: acetonitrile(as 1122-801,Tedia,Fairfield,OH,USA) in water(A) and 0.05% phosphoric acid aqueous solution(B).The column temperature was 30°C and the flow rate was 1.0 ml/min that allowed a gradient to form. UV detection was conducted at 266 nm. Empower software (Shimadzu)was used to collect and analyze chromatographic data.

Bacterial strains and culture conditions

The *S.pn* strain D39[40] was cultured at 37°C in Todd Hewitt broth then the culture was inoculated onto Tryptic Soy Broth (TSB) agar plates and incubated under the same conditions overnight. Next, the bacterial fluid was collected from the plates and cultured in Todd Hewitt broth supplemented with 5% yeast extract until growth reached mid-log phase(as determined by optical density at 600 nm).

e-ISSN: 2320-3528
p-ISSN: 2347-2286

Animals

Female BALB/c mice, which had been housed and maintained for 6 weeks until they weighed 20±2 gm, were purchased from the Experimental Animal Center of Changchun University of Traditional Chinese Medicine. The mice were allowed to rest for 5 days to acclimate before being subjected to experimental manipulations, with all procedures complying with guidelines set forth by the Animal Care and Use Committee (ACUC) affiliated with the Changchun University of Traditional Chinese Medicine. 24 mice were randomly divided into 4 groups: Control group, *S.pn* group, *S.pn* + QFY(L)group(0.42 g/kg), and *S.pn*+QFY(H)group(0.84 g/kg),where (L) denotes Low-Dose and (H) denotes High-Dose QFY. Pneumonia was induced according to previously reported experimental methods[41]. Briefly, mice in *S.pn*, *S.pn*+QFY(L), and *S.pn*+QFY(H) groups were lightly anesthetized by inhalation of isoflurane then were infected with a 25 µL volume of nose drops containing 2.5×108 CFU/ml of *S.pn* to achieve an *in vivo* pneumonia model. Meanwhile, mice in *S.pn*+QFY(L) and *S.pn*+QFY(H) groups were administrated QFY by means of intragastric administration twice daily. In these experiments, all mice were sacrificed at 48 hr post-infection.

Hematoxylin-Eosin (HE) staining of lung tissues

Lung tissues of mice were prepared for histology and analyzed as described earlier [41] by immersing them in 4% paraformaldehyde followed by paraffin embedding, sectioning, and dewaxing of slices with xylene, with ethanol washes performed between steps. After water was removed via dehydration, slices were stained with hematoxylin for 5 min. After rinsing slices in hydrochloric acid ethanol rinse(differentiation step) for 30 sec, slices were soaked in distilled water for 15 min, immersed in eosin staining solution for 2 min, then dewaxed until transparent and sealed. To score lung inflammation and damage, the entire lung surface was analyzed with respect to the following parameters- interstitial damage, vasculitis, peri-bronchitis, edema, thrombus formation and pleuritis. Each parameter was graded on a scale of 0–4 (0-absent; 1-mild; 2-moderate; 3-severe; 4-very severe)[42,43]. Percentages of lung surfaces exhibiting signs of pneumonia were scored and graded according to the following scale:
0–4(0: absent; 1:5–20% confluent pneumonia; 2:21–40%; 3:41–60%; 4:61–80%; 5:81–100%). The total lung inflammation score was expressed as the sum of the scores for each parameter, with a maximum attainable score of 24[44].

Bronchoalveolar lavage

Briefly, the trachea was exposed through a midline incision and Bronchoalveolar Lavage Fluid(BALF) was harvested by instilling and retrieving two 0.5ml aliquots of sterile isotonic saline[42]. BALF was centrifuged at 3000 rpm for 5 min, frozen at 234-280°C, then was analyzed via ELISA for inflammatory factors such as IL-6, IL-1β and TNF-α.

e-ISSN: 2320-3528
p-ISSN: 2347-2286

Quantitative proteomics analysis

Proteomics analysis was conducted by Jingjie PTM BioLabs(Hangzhou, China). Primary experimental procedures for 4D Label free proteomics analysis included protein preparation, trypsin digestion, HPLC fractionation, LC-MS/MS analysis and bioinformatics analysis.

Protein extraction and digestion

Proteins were extracted from lung tissues of mice in Control, *S.pn* and *S.pn*+QFY groups as previously described[45]. Briefly, after each sample was frozen in liquid nitrogen, it was ground into a powder to which lysis buffer (8M urea, 1% Protease Inhibitor Cocktail) was added followed by three rounds of sonication on ice using a high-intensity ultrasonic processor (Scientz, China). Remaining debris were removed by centrifugation at 12,000 × g at 4°C for 10 min. Finally the supernatant was collected and the protein concentration was determined using a BCA kit according to the manufacturer's instructions.

Quantitative proteomic analysis by LC-MS/MS and data analysis

The tryptic peptides were dissolved in solvent A(0.1% FA, 2% ACN in water)and were separated on a home-made analytical column(25 cm length,100 μm i.d.)with a gradient from 4% to 22% solvent B(0.1% FA in ACN) over 70 min, 22% to 30% in 14 min, 80% in 3 min, then equilibrated for 3 min. All at a flow rate of 450 nL/min on a nano Elute UHPLC system(Bruker Daltonics).The peptides were subjected to Capillary source followed by the tims TOF Pro (Bruker Daltonics)mass spectrometry. Precursors with charge states 0 to 5,and fragments MS/MS scan range from 100 to 1700 m/z were analyzed at the TOF detector and 10 PASEF-MS/MS scans were acquired per cycle. The resulting MS/MS data were processed using MaxQuant(v.1.6.6.0)with integrated Andromeda search engine. Tandem mass spectra were searched against Swissprot Mouse database(17032 entries)concatenated with reverse decoy database.False discovery rate for protein,peptide was adjusted to 1%.

Bioinformatics analysis

In the present study, ontology-based pathway analysis was conducted using the Gene Ontology(GO)Consortium-based vocabulary of terms. Subcellular localization prediction, functional enrichment and cluster analysis were all performed using GO terms and KEGG pathways. Cluster membership was visualized using a heat map developed using the"heatmap.2" function from the "plots" R-package. Fold changes in protein levels for Control, S.pn, and S.pn+QFY group comparisons were calculated as mean values according to relative and absolute quantification ratios of protein isobaric tags. Student's t-tests were conducted using SPSS 25.0 to assess statistical significance of results,with proteins exhibiting significant differential expression($p<0.05$)with an expression fold-change>2 identified as differentially expressed biomarkers.

Western blot analysis

Western blot analysis of proteins obtained from lysates of cells or lung tissue homogenates were performed as described previously[46]. 30 μg of each lysate was separated/lane using 10% SDS-PAGE gels. Primary antibodies specific for the following antigens were used at 1:1000 dilution:β-tubulin,GAPDH,NLRP3,ASC,cleaved-casp1, LC3B,

e-ISSN: 2320-3528
p-ISSN: 2347-2286

P62 p-mTOR, mTOR,p-ULK,ULK,NF-κB p65,p-NF-κB p65,andIκB. After blots were incubated with primary antibodies overnight at 4°C, they were incubated with secondary horseradish peroxidase-conjugated IgG (either goat anti-mouse or goat anti-rabbit) diluted 1:5000. Protein bands were visualized and analyzed using a chemiluminescent imaging system (FluorChem, ProteinSimple, San Jose, CA, USA).

Immunohistochemistry

Immunohistochemistry was performed on mouse lung tissues after they were paraffin-embedded, sectioned and deparaffinized, hydrated and heated in a low-pH citrate buffer using a microwave oven to render intracellular antigens accessible to immunostaining. Subsequently sections were separately immunostained with rabbit polyclonal antibodies overnight at 4°C.Next, sections were submerged in a hydrogen peroxide solution for 5 min at room temperature to block endogenous peroxidase activity followed by treatment with corresponding fluorescent antibody for 60 min at room temperature. Fluorescently stained sections were then counterstained with DAPI solution(nuclear staining)for 5 min then were dried and sealed with a reagent to prevent fluorescence quenching during storage. Sections were observed under a Nikon inverted fluorescence microscope(Nikon Eclipse Ti-SR, Nikon, Japan)and images were captured with a DS-U3 system(Nikon).

Cell culture

MH-S cells of 5th passage were cultured at 37°C in 5% CO_2 in 1640 medium supplemented with 10% FBS and 1% penicillin-streptomycin. In vitro experimental groups included Control, PLY, PLY+QFY, PLY+QFY+3-MA, PLY+QFY+MCC950 groups. MH-S cells were stimulated with purified PLY(1 μg/mL)to generate the in vitro lung injury model then cells were treated with QFY(25 μg/mL) for 48 hr followed by treatment with or without 3-MA(10 ng/mL) or MCC950(10 μg/mL) for 1 hr before cells were collected for further analysis.

Statistical analysis

All data are presented as means ± SD as calculated using Student's t-test Comparisons between groups were conducted using one-way or two-way ANOVA followed by Bonferroni or Tukey's post-tests as indicated. Differences were considered significant at Control group vs *S.pn* group, #P<0.05,##312 P<0.01, *S.pn* group vs *S.pn*+QFY,*P<0.05, **P<0.01, with n.s. used to indicate results were not significant.

RESULTS

HPLC chromatograms of QFY formulations

HPLC-MS/MS methods have been widely used to analyze major compounds in various herbal medicines. In this study,19 main compounds of QFY were identified simultaneously. The Total Ion Current (TIC) of these 19 components were shown in (Figure 1a-1b).For the exact identification of QFY compound discoverer 3.1 was used for retention time correction, peak identification and extraction. Information about the compound's name, molecular formula, Retention Time (RT), mass accuracy and adduct were listed in Table 1. Consistent with HPLC-MS/MS result, 14 main peaks in the HPLC fingerprint were attributed to QFY compounds (Figure 1c). Due to the fact that the proportion of the Cytidine, Adenosine, Caffeic acid, Phillyrin, monopalmitin were very low, the peaks of them were not identified in the HPLC, and they were not used as a reference for similarity evaluations. Finally, ten batches of QFY recipe were compared and analyzed. All the compounds similarities were within the range of 95% to 98%. Above results indicated that QFY retained the principal active component of four Chinese herbs, and formulations exhibited good repeatability (Figure 1d).

e-ISSN: 2320-3528
p-ISSN: 2347-2286

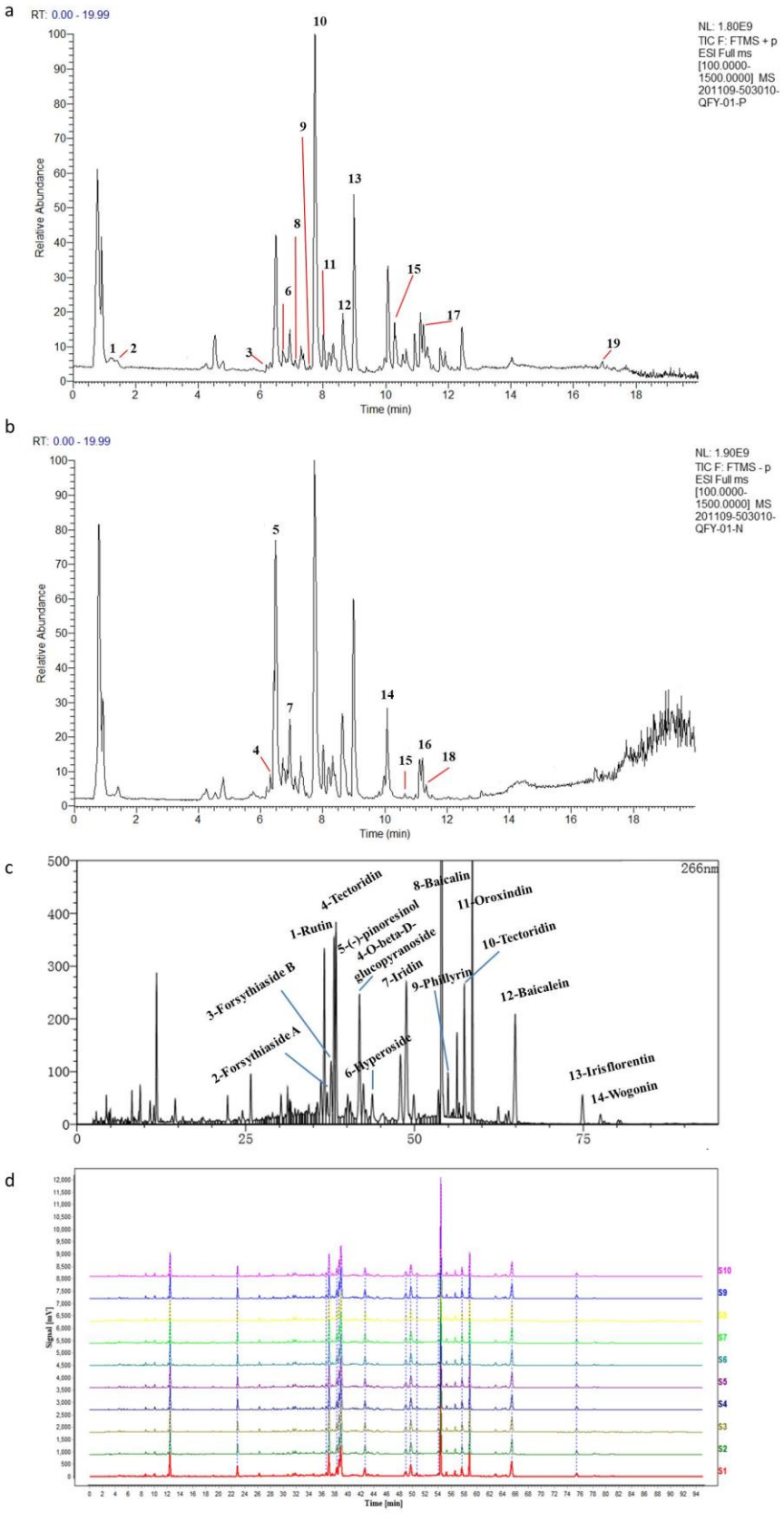

e-ISSN: 2320-3528
p-ISSN: 2347-2286

Figure 1: HPLC chromatogram of QFY formulation (a,b)Total Ion Current (TIC) of QFY 820 formulation extracts in both positive and negative ion models, (c) HPLC chromatogram of QFY formulation, (d) HPLC fingerprint chromatograms of 10 batches of QFY (S1–10) formulations analyzed using National Pharmacopeia Committee Chinese Medicine Fingerprint Similarity Evaluation System (2004A) software, with UV detection at 266 nm.

Table 1. In the compound discoverer 3.1 library for the analysis of 19 compounds using UPLC-MS/MS.

No	RT (min)	Ginsenosides	Molecular formula	Expected neutral mass(Da)	Observed neutral mass(Da)	LC/MS (ESI-) (m/z)	Mass accuracy (ppm)	Adducts
1	1.189	Cytidine	$C_9H_{13}N_3O_5$	243.08544	243.08552	244.0926	-0.33	$[M+H]^+$
2	1.588	Adenosine	$C_{10}H_{13}N_5O_4$	267.09645	267.09675	268.10279	-1.12	$[M+H]^+$
3	6.113	Caffeic acid	$C_9H_8O_4$	180.04215	180.04226	181.04947	-0.61	$[M+H]^+$
4	5.792	Caffeic acid	$C_9H_8O_4$	180.04214	180.04226	179.03421	-0.62	$[M-H]^-$
5	6.345	Forsythoside B	$C_{34}H_{44}O_{19}$	756.24826	756.24768	755.24115	0.77	$[M-H]^-$
6	6.522	Rutin	$C_{27}H_{30}O_{16}$	610.15381	610.15338	609.14642	0.70	$[M-H]^-$
7	6.82	Forsythoside A	$C_{29}H_{36}O_{15}$	624.20518	624.20542	625.21252	-0.38	$[M+H]^+$
8	6.983	(-)-pinoresinol 4 O-beta-D glucopyranoside	$C_{26}H_{32}O_{11}$	520.19442	520.19446	519.18713	-0.08	$[M-H]^-$
9	7.058	Hyperoside	$C_{21}H_{20}O_{12}$	464.09513	464.09548	465.10214	-0.75	$[M+H]^+$
10	7.661	Iridin	$C_{24}H_{26}O_{13}$	522.13725	522.13734	523.14453	-0.17	$[M+H]^+$
11	7.723	Phillyrin	$C_{27}H_{34}O_{11}$	534.2086	534.210112	535.19586	-2.83	$[M+H]^+$
12	8.093	Baicalin	$C_{21}H_{18}O_{11}$	446.08431	446.08491	447.09115	-1.34	$[M+H]^+$
13	8.729	Tectoridin	$C_{22}H_{22}O_{11}$	462.11591	462.116212	463.12323	-0.65	$[M+H]^+$
14	8.986	Oroxindin	$C_{22}H_{20}O_{11}$	460.10008	460.10056	461.10733	-1.04	$[M+H]^+$
15	10.118	Baicalein	$C_{15}H_{10}O_5$	270.0528	270.05282	269.04553	-0.07	$[M-H]^-$
15	10.03	Tectorigenin	$C_{16}H_{12}O_6$	300.06326	300.06339	299.05588	-0.43	$[M-H]^-$
16	10.341	Tectorigenin	$C_{16}H_{12}O_6$	300.06308	300.06339	301.01037	-1.03	$[M+H]^+$
17	11.197	Chrysin	$C_{15}H_{10}O_4$	254.05766	254.05791	253.05038	-0.98	$[M-H]^-$
18	11.283	Irisflorentin	$C_{20}H_{18}O_8$	386.09958	386.100168	387.10693	-1.52	$[M+H]^+$

e-ISSN: 2320-3528
p-ISSN: 2347-2286

19	11.384	Wogonin	$C_{16}H_{12}O_5$	284.06839	284.06847	283.0611	-0.28	$[M-H]^-$
20	17.467	monopalmitin	$C_{19}H_{38}O_4$	330.27645	330.27701	331.28357	-1.69	$[M+H]^+$

Note: $[M+H]^+$, $[M-H]^-$ are molecular ions observed in positive and negative ion chemical ionization mass spectra respectively.

Impact of QFY on lung pathology and inflammatory cytokines in S.pn-induced pneumonia mouse model

S.pn, S.pn + QFY(L), and S.pn + QFY(H) groups of mice were inoculated with 2.5×10^8 CFU/mL S.pn in 25 µL 48 hr post-infection. Histological changes in lung tissues of mice were examined to evaluate the protective effect of QFY against the development of a pulmonary inflammatory response *in vivo*. Representative lung histology of mice showed extensive signs of pneumonia, with deepened color of lung tissue accompanied by interstitial inflammation, vasculitis, bronchitis, and edema. Lobes were congested and swollen and exhibited evidence of neutrophil infiltration. After QFY treatment, lung tissue bleeding and swelling were reduced. Based on the semi-quantitative scoring system described in the Methods section, histopathology scores were much lower in QFY-treated mice, especially for the *S.pn* + QFY (H) group, indicating that QFY treatment of mice prevented lung inflammatory damage induced by *S.pn* (Figures 2a-2c). We measured levels of inflammatory cytokines in BALF to investigate effects of S.pn infection on lung inflammation and protective effects of QFY against S.pn-induced pneumonia. As shown in Fig. 2d-f, S.pn infection led to significantly increased inflammatory cytokine levels of TNF-α, IL-1β, and IL-6 in BALF ($p <$ 0.01). In addition, QFY supplementation significantly decreased levels of IL-1β and TNF-α as compared to corresponding levels in S.pn-infected mice, while IL-6 levels were not significantly decreased ($p>0.05$). Thus, the abovementioned data revealed that S.pn infection induced lung inflammation that was reversed by QFY treatment. Next, the group of *S.pn*+QFY in proteomics and western blotting analysis were refer to High dose QFY (0.84g/kg) treatment if not otherwise mentioned.

e-ISSN: 2320-3528
p-ISSN: 2347-2286

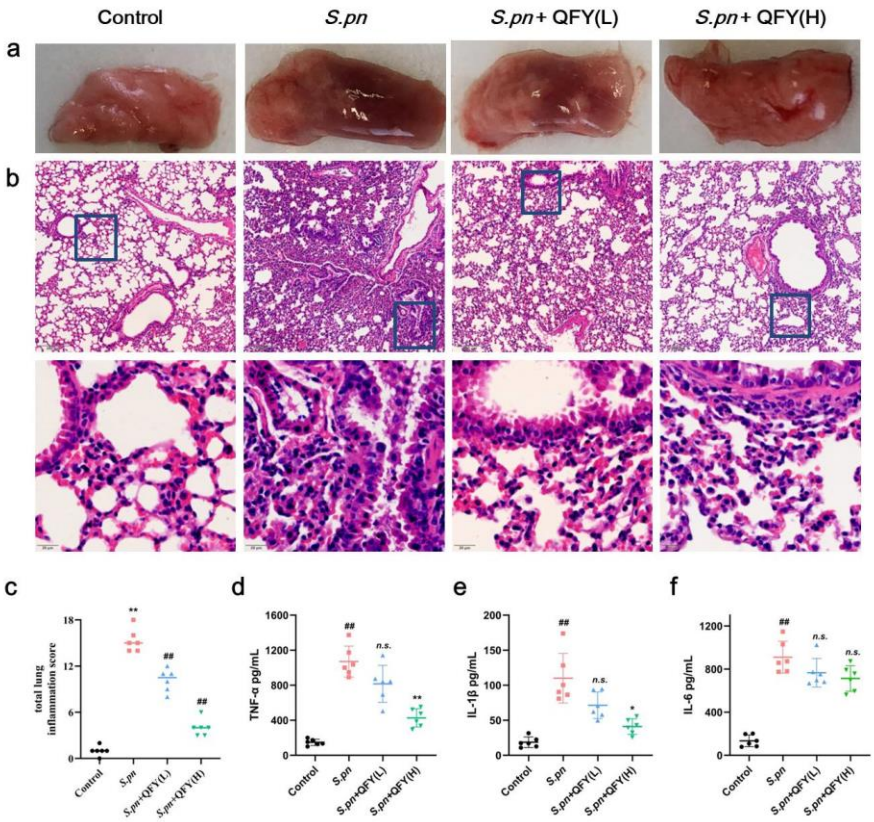

Figure 2. QFY prevented S.pn-induced lung inflammatory injury in infected mice.

(a,b)Pathologic and histopathological changes in lung tissues. Lung tissues stained with H&E (original magnification 40×, scale bar: 20 μm), (c)Total lung inflammation score, (d-f)Influence of QFY on inflammatory factors detected in infected mice.

(Note: Data are presented as means ± SD of n=6 mice per treatment group. #p<0.5, ## p<0.01 versus Control, *p<0.5 **p<0.01 versus S.pn)

QFY treatment alters protein expression in *S.pn*-infected mice

In order to reveal precise molecular mechanisms whereby QFY alleviated S.pn-induced pneumonia in mice, 4D label free quantitative proteomics analysis was used to examine differentially expressed proteins in lung tissues of QFY-treated S.pn-infected mice. Here, repeatability of protein quantitation was evaluated using principal component analysis (PCA) based on Pearson's correlation coefficients. APCA score plot revealed overall classifications among groups (Figure 3a). The tendency of groups to cluster between control and S.pn-infected groups was apparent, with the QFY-treated group (0.84 g/kg) cluster shifting toward the Control group (even though two samples were misclassified together with the S.pn-infected group), indicating QFY treatment was effective. Pearson correlation coefficients of the quantification values (after a log2 transformation) were calculated for all samples and to detect linear correlations between two groups of data. When the Pearson coefficient (r) was closest to -1, data groups were negatively correlated; if r was closest to 1, then data groups were positively correlated; if r was closest to 0, no correlation between data groups was found. (Figure 3b).

e-ISSN: 2320-3528
p-ISSN: 2347-2286

Moreover, the results indicated that the linear correlation was strengthened between Control and QFY-treated groups (r>0.97, with the exception of the *S.pn* + QFY-3 sample). Of the total 5795 proteins that were quantified, 655 differential proteins were identified in the S.pn group versus the Control group (2-fold change cutoff and value of P<0.05), among which 433 proteins were up-regulated and 222 proteins were down-regulated. To further explore biological significance of differentially expressed proteins, proteins were categorized according to GO functional annotation terms. GO enrichment analyses of differentially expressed proteins using a senior bubble chart. Bubble size indicates the number of proteins belonging to a given pathway and the color represents the p-value. (Figures 3c-3d) and were mainly assigned to several biological processes, including regulation of immune and cytokines production, response to bacterium, and defense response. Additionally, 345 proteins were differentially expressed in the QFY-treated group as compared to the S.pn-infected group. As expected, these differentially expressed proteins were significantly enriched during pathogen infection relative to other processes mentioned above. Taken together, these data suggest that QFY significantly reversed S.pn-induced alterations of host defenses and immune response.

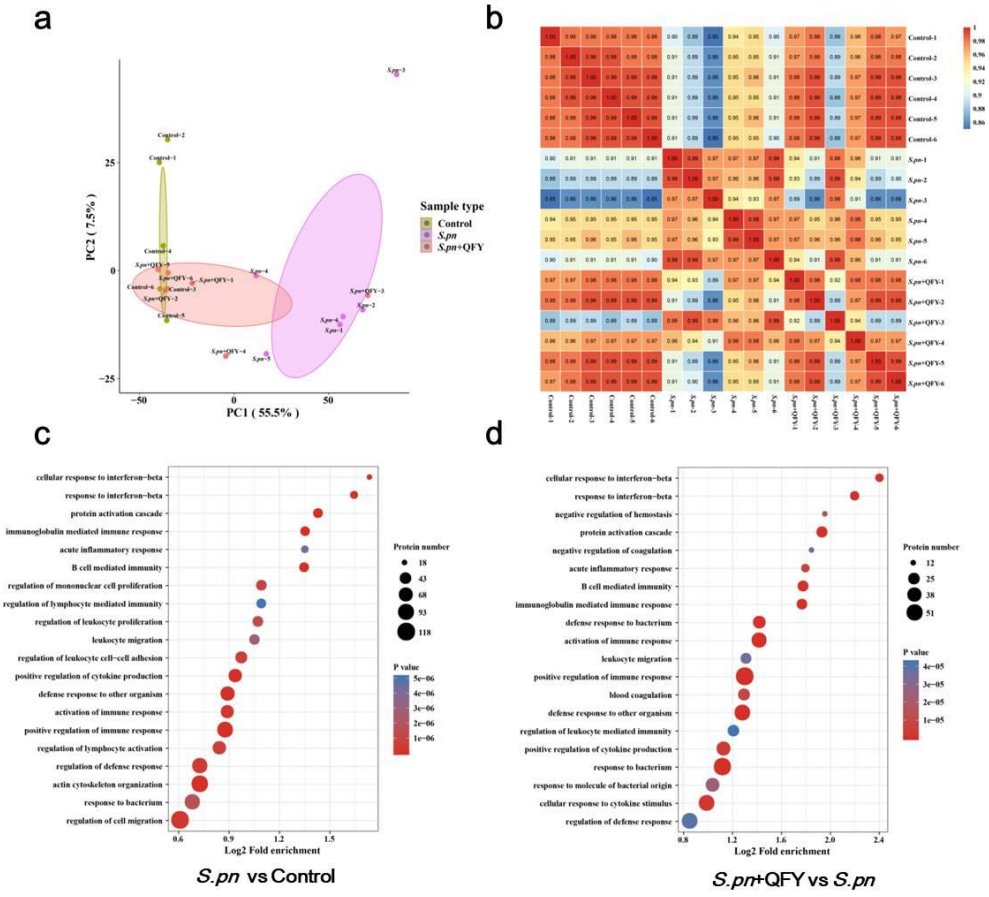

Figure 3. Group classification and GO functional annotation. (a)Overall visualization of group classifications using a PCA score plot, (b)Pearson correlation coefficient analysis, (c,d)GO enrichment analyses.

e-ISSN: 2320-3528
p-ISSN: 2347-2286

QFY treatment alleviates S.pn-induced pneumonia via NOD-like receptor and autophagy signaling pathways

To further investigate the QFY target and QFY mechanism of action during S.pn infection, a KEGG-based biological analysis of differentially expressed proteins was performed. As shown in (Figures 4a-4d), 36 and 13 differential proteins were enriched in NOD-like receptor and autophagy signaling pathways, respectively. Using Western blotting and Immunohistochemistry (IHC), representative differentially expressed proteins were further verified. NLRP3, a well-known NOD-like receptor, is activated by *S.pn* invasion but is significantly down-regulated after subsequent QFY treatment. Notably, NLRP3 and NF-κB signaling pathways jointly participate in cytokines release, thus verifying involvement of other representative proteins in the abovementioned signaling pathways. As shown in (Figure 5a) levels of ASC, cleaved-casp1, and phosphorylated NF-κB p65 proteins were increased after *S.pn* infection, with QFY treatment markedly restoring expression of these proteins to normal levels. Notably, autophagy has emerged as an essential process for maintaining host homeostasis during pathogen invasion[47] [48]. (Figures 5a-5b) and IHC (Figures 5c-5d) in mouse lung tissues of Control, *S.pn*, and *S.pn*+QFY groups (0.84 g/kg). Staining intensities of LC3B, p62, and Lamp2 proteins were calculated relative to DAPI staining results obtained for at least 6 areas of interest, with results pooled from four independent experiments. Statistical analysis was performed using one-way ANOVA followed by Tukey's post-test, with data presented as the mean ± SD for each group, $^{\#}p<0.5$, $^{\#\#}p<0.01$ versus Control, $^{*}p<0.5$ $^{**}p<0.01$ versus *S.pn*. As shown in (Figure 5b), mTOR-dependent autophagy was inhibited, as evidenced by mTOR phosphorylation and p62 accumulation at 48 hr post-S.pn infection (Figures 5c-5d). Moreover, altered autophagy observed after *S.pn* infection was further supported by observations of decreased LC3B and increased Lamp 2 fluorescence intensities (Figures 5c-5d). Conversely, QFY treatment enhanced host defense capacity by promoting autophagy, as indicated by QFY blockage of mTOR phosphorylation and restoration of LC3B levels that had decreased after S.*pn* infection. Corroboration of the abovementioned data indicates that QFY alleviated *S.pn*-induced pneumonia by inhibiting activation of NLRP3 inflammasomes and by repairing defective autophagy. We speculate that QFY may exert a similar protective effect in *in vivo* experiments even in the absence of direct exposure to intact *S.pn* organisms, prompting us to test this hypothesis by studying PLY-treated MH-S cells as an in vitro pneumonia model.

e-ISSN: 2320-3528
p-ISSN: 2347-2286

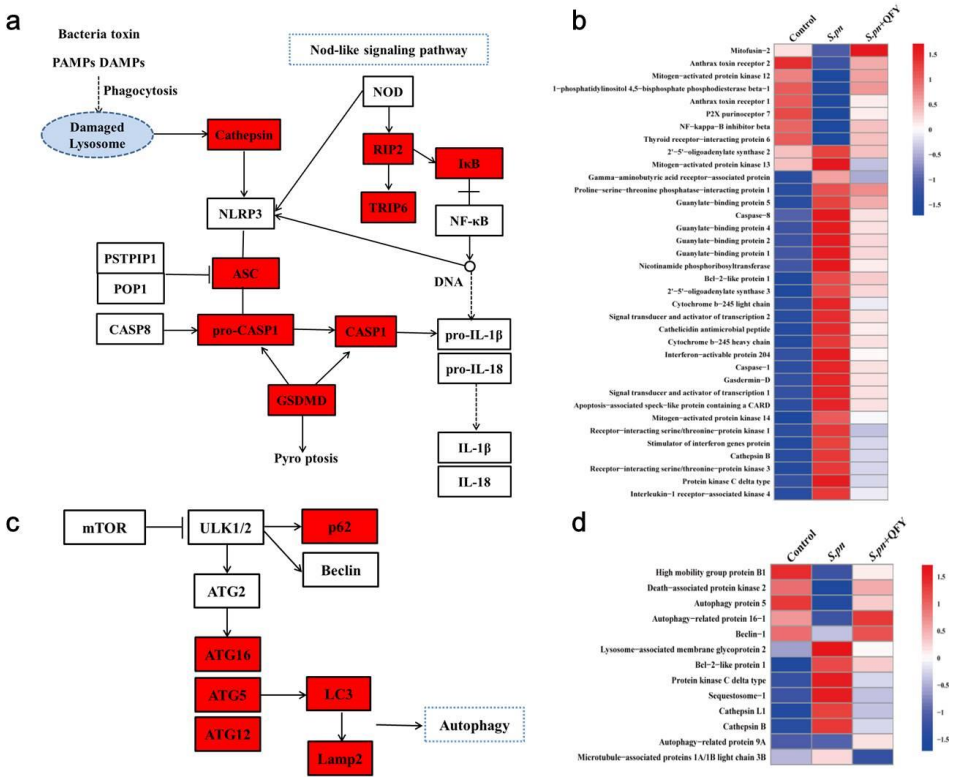

Figure 4. QFY alters expression of NOD-like receptor and autophagy signaling pathways. (a,c)KEGG interaction network diagram of NOD-like receptor and autophagy signaling pathway (red indicates differentially expressed proteins), (b,d)Heat maps of differentially expressed proteins of NOD-like receptor and autophagy signaling pathways (n=6).

(Note: Proteins were extracted, separated, and identified using LC-MS/MS analysis)

e-ISSN: 2320-3528
p-ISSN: 2347-2286

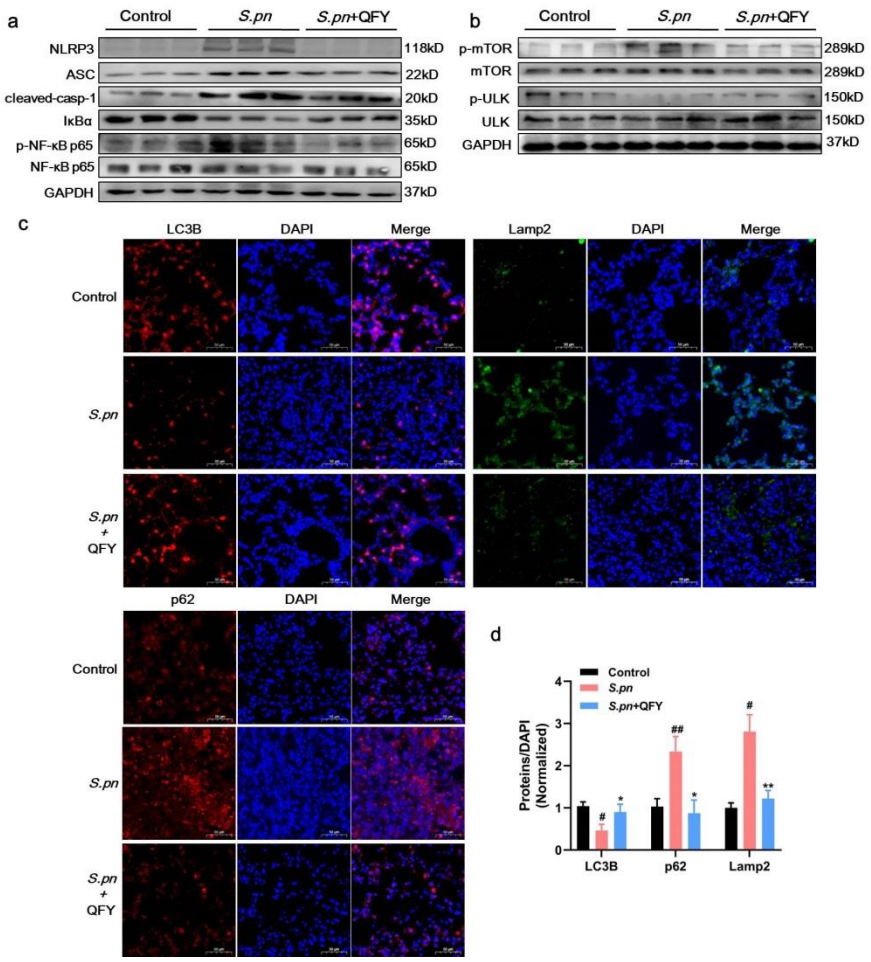

Figure 5. Validation of expression of key proteins associated with NLRP3 inflammsomes, autophagy and NF-kB signalling pathways using Western blot analysis.

Effect of QFY on PLY-induced MH-S cells

PLY triggering of cell death and its role in evasion of several host defense mechanisms appear to directly activate NLRP3 inflammasomes during *streptococcus* infection[49]. To further explore whether QFY protective alleviation of S.pn infection was associated with NLRP3 inhibition (and autophagy activation as well), we investigated expression levels of key proteins within PLY-treated MH-S cells. Here, MH-S cells were stimulated with PLY (400 ng/mL) for 24 hr followed by low-dose (25 μg/mL) or high-dose (50 μg/mL) QFY treatment. MH-S cells were stimulated with PLY (400 ng/mL) for 24 hr then treated with low-dose QFY (25 μg/mL) or high-dose QFY (50 μg/mL). Proteins were quantified and data are presented as mean ± SD for each group (n=3), $^{\#}p<0.5$, $^{\#\#}p<0.01$ versus Control, $*p<0.5$ $**p<0.01$ versus S.pn. (Figure 6). Concurrent with *in vivo* experimental results, activation of NLRP3 inflammasomes was reinforced by increases in levels of NLRP3, ASC, and cleaved-casp1 proteins, with dysfunctional autophagy also detected, as revealed by increased mTOR phosphorylation and p62 accumulation. Concomitant with autophagy inhibition, the NF-κB signaling pathway was activated, as confirmed by the observed

e-ISSN: 2320-3528
p-ISSN: 2347-2286

reduction of IκBα (decreased by 31.33% compared with the Control group) and by phosphorylation of NF-κB p65 (increased by 66.7% compared with the Control group) that together intensified the inflammatory cascade. Taken together, the abovementioned results indicate that the QFY therapeutic effect is linked to reduction of NLRP3 and activation of autophagy. Importantly, it has been reported that NLRP3 and autophagy pathways are linked by reciprocal regulation[50-52]; mechanistically, autophagy is essential for NLRP3 inflammasome degradation, while NLRP3 can act as a novel inhibitor of autophagy[33]. These observations inspired us to further explore bidirectional regulatory mechanisms involving NLRP3 and autophagy pathways and to identify QFY targets.

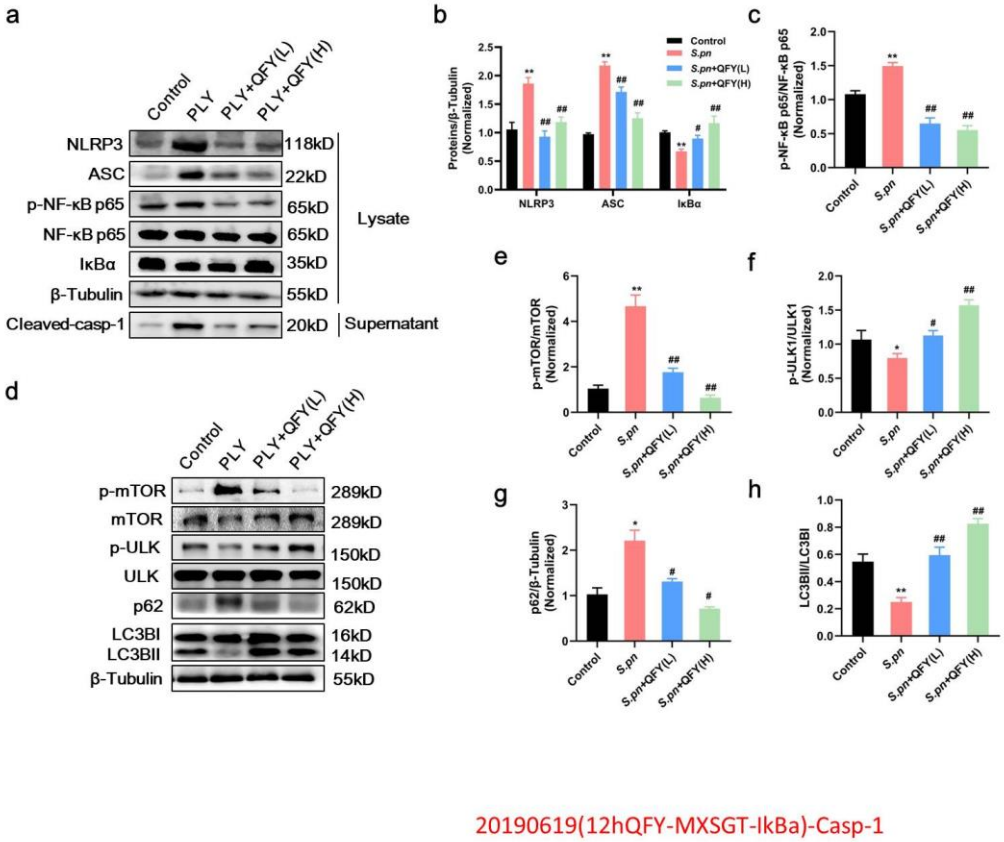

20190619(12hQFY-MXSGT-IkBa)-Casp-1

Figure 6. QFY reduced NLRP3 inflammsomes, NF-kB signalling pathways and induced autophagy in PLY stimulated MH-S cells.

QFY activates autophagy by down-regulating upstream NLRP3/mTOR pathways.

Mounting evidence has revealed that NLRP3 acts as a binding partner of mTOR that together inhibit autophagy[33] and, in turn, autophagy is essential for NLRP3 inflammasome degradation[32]. Spearman correlation analysis was performed to assess the potential association between autophagy and the NLRP3 inflammasome. Intriguingly, a highly significant positive correlation was observed between autophagy-related protein tool lung inflammatory scores (TLISs) and levels of inflammatory cytokines IL-1β and TNF-α. Conversely, NLRP3, ASC, and cleaved-casp1 levels were significantly positively correlated with p-mTOR/mTOR and p62 levels and significantly negatively correlated with LC3BII/I, Beclin, Atg5, and p-ULK/ULK levels (Figure 7a). Taken together, these findings indicate

e-ISSN: 2320-3528
p-ISSN: 2347-2286

that development of pneumonia is accompanied by blockage of autophagy, with NLRP3 inflammasome and autophagy pathways negatively associated with one another. Next, the response of MH-S cells against PLY stimulation (400 ng/mL) was explored through time-course experiments conducted from 6 hr to 48 hr. As shown in (Figure 7b-d), protein expression levels of NLRP3 and ASC were not significantly altered at 6 hr post-infection. However, after prolonged infection of 48 hr duration, expression of NLRP3 and ASC increased more than 3-fold as compared with their respective basal levels. As expected, PLY treatment induced transiently increased autophagy after 6 hr as a defense response; this response was significantly reduced as NLRP3 continued to accumulate, as evidenced by a decrease of LC3BII/LC3BI by 59.02% as compared with the Control group. Since our abovementioned results suggest a protective effect of QFY and reciprocal regulation of NLRP3-autophagy, we sought to elucidate the exact molecular target of QFY using NLRP3 inhibitor MCC950 and the PI3K inhibitor 3-Methyladenine (3-MA), an autophagy inhibitor. Concurrent with our above mentioned data, QFY treatment significantly down-regulated NLRP3 pathway activity and also repaired defective autophagy. y. MH-S cells were stimulated with purified PLY (400 ng /mL) to induce the lung injury model then were treated with QFY (25 μg/mL) for 48 hr followed by treatment with 3-MA (10 ng/mL) or MCC950 (10 μg/mL) 1 h before cells were collected. (Figure 8a), while 3-MA inhibited the autophagy response, as indicated by increased p62 and decreased LC3B levels as shown in (Figure 8a). Notably, treatment with QFY reversed the PLY-induced increase in NLRP3 pathway member levels even in the presence of 3-MA. Thus, these results suggest that QFY suppressed the PLY-induced inflammatory response by inhibiting NLRP3 activation rather than by triggering the autophagy pathway, whereby the latter would have promoted p65 phosphorylation to initiate an inflammatory cascade. Next, we further explored whether NLRP3 is the target of QFY modulation of autophagy and amelioration of inflammation. As shown in (Figure 8e) the silencing of NLRP3 by MCC950 markedly restored the basal autophagy level through inactivation of mTOR, reinforcing the hypothesis that NLRP3 degradation preceded and triggered activation of autophagy [33]. In summary, the QFY anti-*streptococcus pneumonia* effect appears to be associated with activation of autophagy through down-regulation of upstream autophagy pathway events involving NLRP3/mTOR.

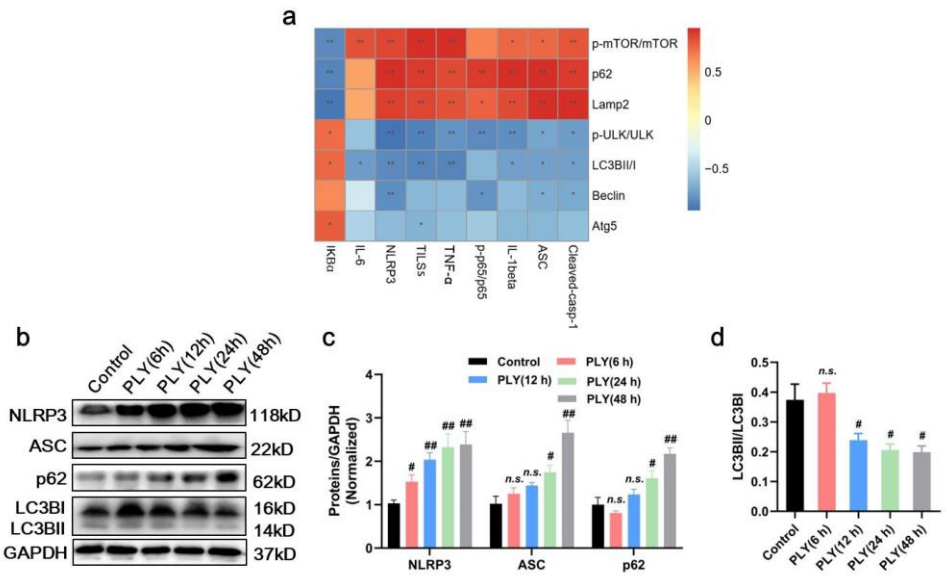

e-ISSN: 2320-3528
p-ISSN: 2347-2286

Figure 7. (a)Spearman correlation analysis of autophagy and NLRP3 inflammasome signaling pathways, (b)The response of MH-S cells against PLY stimulation (400 ng/mL) was explored through a time-course experiment conducted from 6 hr to 48 hr post-stimulation, (c,d)Proteins were quantified in with data are presented as mean ± SD for each group (n=3), #p<0.5, ## p<0.01 versus Control.

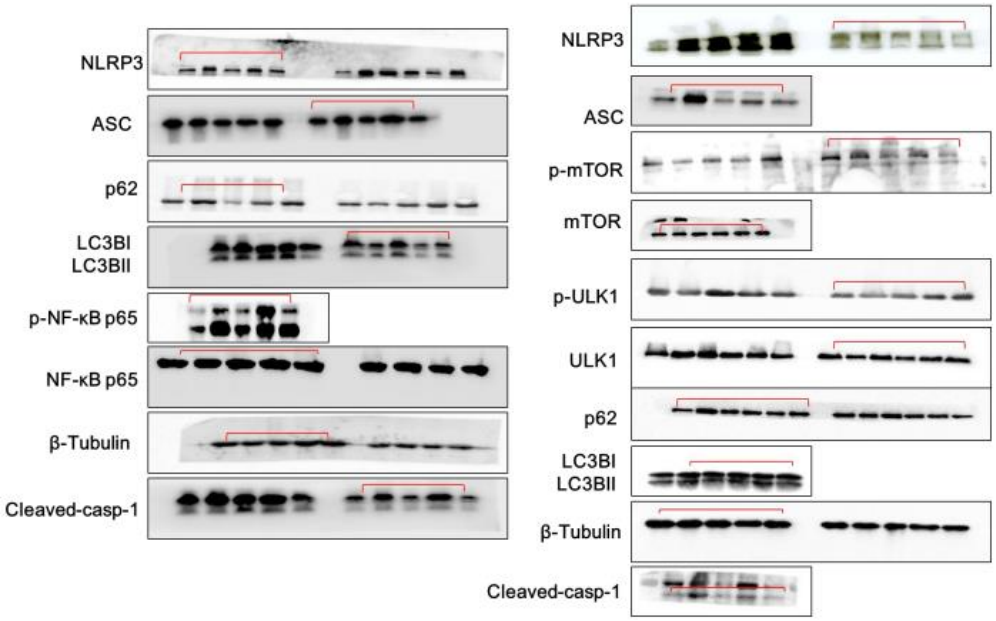

Figure 8. QFY activates autophagy by down-regulating the upstream NLRP3/mTOR pathway. (a,e)Protein expression detected by Western blotting. (b,c,d)Proteins were quantified,(f,g,h,i)Data are presented as the mean ± SD for each group (n=3), #p<0.5, ##p<0.01.

DISCUSSION

Major conclusions of this study can be summarized as follows: first, QFY exerts prominent anti-pneumonia effects both in a S.pn-induced *in vivo* mouse model and an in vitro PLY-stimulated MH-S cell-based model. Secondly, 4D Label free proteomics analysis showed that suppression of NLRP3 inflammasome activity and repair of autophagy played pivotal pharmacological roles in QFY pneumonia therapy. Finally, our date and previous researches demonstrated that NLRP3 and autophagy were linked by reciprocal negative regulation processes. QFY triggered autophagy through down-regulation of upstream NLRP3/mTOR signaling pathway events, resulting in quenching of the NF-κB pathway and amelioration of inflammatory injury.

Global Burden of Diseases, Injuries, and Risk Factors Study (GBD) reported lower respiratory tract infections resulted in 2.38 million deaths in 2016. Among children, those younger than 5 years of age accounted for 27.45% of lower respiratory infection deaths. *Streptococcus pneumoniae* induced Pneumonia was main cause of lower respiratory tract infections, which contributing to more than 1.189 million deaths per year[53].

Nowadays, antibiotic resistance has led to the declining effectiveness of traditional antimicrobial agents used to combat *S.pn* infections, necessitating the development of strategies for reducing antibiotics application [54, 55]. TCM

e-ISSN: 2320-3528
p-ISSN: 2347-2286

has been practiced for thousands of years and is widely recognized as therapeutically curative when used for treatment of several diseases and physiological conditions[56]. In fact, treatment efficacies of some TCM-based approaches have been experimentally confirmed[57-60]. According to the theory of TCM, "heat toxin" is closely related to pneumonia. QFY is derived from the Gan Lu Xiao Du pill, a famous classic recipe with the effect of dampness and heat removing and detoxifying, and it is known for its efficacy for the treatment of pneumonia. *Sacutellaira baicalensis*, *Belamcandae Rhizoma* and *Forsythia* is the main compounds of QFY. Among them, Baicalin[58,61], Phillyrin [61], and *Forsythia suspensa*, possess antibacterial and anti-inflammatory activities, while *Scutellariae radix* has been reported to inhibit cancer cell growth and attenuate inflammation[63] .Because of their variability and complexity, efficacies of Chinese herbal compounds have been frequently questioned, due to the lack of rigorous scientific evidence supporting their effectiveness. Thus, studies of TCM herbal compound QFY that align with biomedical perspectives are pivotal to its acceptance in clinical settings. Therefore, we established *S.pn*-infected mouse-based and PLY-stimulated MH-S cell-based lung infection models to investigate the mechanism underlying QFY protective effects against pneumonia.

HE staining of lung tissues of mice with *S.pn*-induced pneumonia showed extensive signs of infection, such as congested and swollen lobes accompanied by neutrophil infiltration. However, QFY could significantly impact pathological manifestations of lung infection and reduce levels of cytokines IL-1β and TNF-α, with the exact mechanism of action of QFY discussed in detail below.

High-throughput proteomics tools are widely recognized as valuable for use in exploring pharmacology of complex TCM systems [17-19]. Here we identified 36 and 13 differentially expressed proteins that were enriched for NOD-like receptor and autophagy signaling pathways, respectively. Autophagy is an essential homeostatic process which is triggered by danger signals, including pathogen invasion. In line with recent studies linking autophagy and infectious disease[63], our results suggest that lung inflammatory injury reflects deficient autophagy, as demonstrated by p62 accumulation and decreased LC3B levels. Conversely, several research studies have demonstrated that *S.pn* stimulates autophagy during the early phase of infection [63]. We hypothesized that these results reflect differing responses to S.pn at different infectious disease time points, prompting us to investigate this discrepancy by conducting a time-course experiment. Subsequently, it is obviously that autophagy was slightly increased at 6 hr post-infection, thus reflecting its defense response role. However, autophagy decreased with prolongation of infection duration, especially after 48 hr of infection. Interestingly, reduction of autophagy was accompanied by constitutive NLRP3 accumulation.

In lung tissues during early pneumococcal pneumonia, NLRP3 inflammasomes appear to play an increasingly important role in protective immunity as infection duration and bacterial burden increase. This scenario may involve NLRP3 recruitment of adaptor protein ASC followed by pro-caspase-1 recruitment, which then leads to triggering of caspase-1 activation and the cytokines maturation. Interestingly, it has been reported that both Nlrp3−/− and Asc 541 −/− mice exhibit strongly improved host defenses (as compared to mice with functional alleles for each gene) with markedly reduced mortality rates and diminished bacterial growth and dissemination[63]. Importantly, recognition of pneumococcal peptidoglycan and DNA by the NOD-like pathway depends on expression of PLY, which is a well-known and important *S.pn* virulence factor. PLY acts by creating transmembrane pores to cause cell lysis and necrosis of pulmonary epithelial cells and macrophages [63]. Consequently, the immune system employs various distinct types of inflammasomes to sense PLY-induced cellular membrane damage [63].

e-ISSN: 2320-3528
p-ISSN: 2347-2286

Collectively, it is suggested that *S.pn* infection activated NLRP3 and markedly inhibited autophagy. By contrast, QFY-treatment significantly inhibited the NLRP3 signaling pathway, as evidenced by decreases in NLRP3, ASC, and cleaved-casp1 levels, while restoring defective autophagy through mTOR dephosphorylation and p62 degradation. Unexpectedly, the abovementioned data revealed mechanistic parallels between signaling pathways leading to NLRP3 inflammasome activity and autophagy during QFY treatment. Indeed, our results may align with results of several previous studies suggesting that autophagy blockade led to accumulation of damaged ROS-generating mitochondria and subsequent NLRP3 inflammasome activation [51], while triggering of autophagy induced NLRP3 degradation. In turn, NLRP3 was identified as a binding partner of mTOR that inhibited autophagy by promoting mTOR phosphorylation[33].

To further explore the precise targets of QFY regulation of NLRP3 and autophagy, we chose MCC950 and 3-MA as specific inhibitors, respectively. Our results confirmed that QFY treatment reversed PLY-induced NLRP3 pathway activation even in the presence of autophagy inhibitor 3-MA, while the NLRP3 inhibitor MCC950 mimicked QFY action by triggering mTOR-dependent autophagy. Notably, mTOR, a highly conserved serine/threonine protein kinase consisting of two mTOR complex forms, seems to be the biochemical link between NLRP3 and autophagy signaling pathways, as shown in (Figure 9).

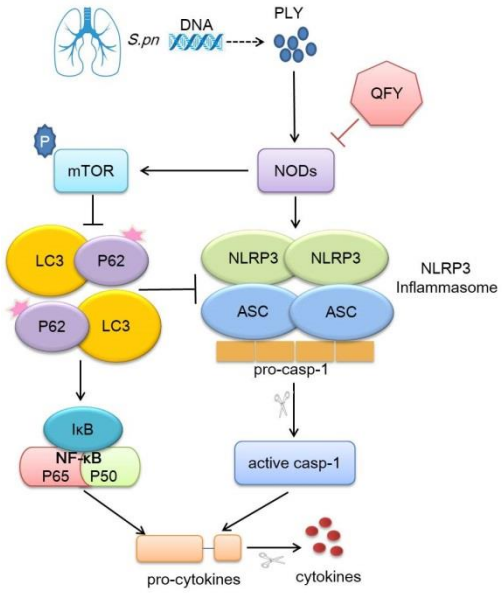

Figure 9. Biochemical link between NLRP3 and autophagy signaling pathways.

In summary, our results demonstrate that NLRP3 inhibited autophagy by binding to mTOR, while QFY reversed infection-impaired autophagy through down-regulation of NLRP3. As a consequence of activated autophagy, the inflammatory cascade induced by the NF-κB signaling pathway was significantly inhibited. This study provides a rationale warranting future investigations into precise targets and mechanisms of QFY and other Chinese herbal remedies for treating lung infectious diseases

CONCLUSION

e-ISSN: 2320-3528
p-ISSN: 2347-2286

In conclusion, the current study has shown that inhibited activity of phagocytes caused by flaxseed was eliminated by the addition of lactobacilli, moderate to significant activation of the local gut as well as total cellular immune response, and improved effect of circoviral vaccine was observed after addition of probiotic lactobacilli and/or flaxseed into the diet of weaned pigs.

ACKNOWLEGEMENT

This work was supported by the National Key Research and Development Program of China (No. 2017YFC1703202), the Jilin Scientific and Technological of Chinese Medicine Program (No. 2019023), the Inheritance and Innovation of Chinese Medicine of “Millions of Standouts” Project (the Project of Qihuang), the Inheritance Workroom of the Chinese Medicine Master Wang Lie, and the Jilin Scientific and Technological Program of Sanitation and Population Control (No. 2018J106) authorized support.

REFERENCES

1) Rudan I,et.al.Epidemiology and etiology of childhood pneumonia. Bull World Health Organ. 2008;86:408-16
2) GBD Diarrhoeal Diseases Collaborators. Estimates of global, regional, and national morbidity, mortality, and aetiologies of diarrhoeal diseases: a systematic analysis for the Global Burden of Disease Study 2015. Lancet Infec Dis.2017;17:909-948.
3) Bernstein J M, et.al. Treatment of community-acquired pneumonia--IDSA guidelines.Chest.1999;115:9S-13S.
4) Bewley M A, et.al. Pneumolysin Activates Macrophage Lysosomal Membrane Permeabilization and Executes Apoptosis by Distinct Mechanisms without Membrane Pore Formation, Mbio.2014; 5:e01710-e01714.
5) Subramanian K, et.al.Pneumolysin binds to the mannose receptor C type 1 (MRC-1) leading to anti-inflammatory responses and enhanced pneumococcal survival, Nat Microbio.2019;4:62-70.
6) Lehtinen S, et.al.Horizontal gene transfer rate is not the primary determinant of observed antibiotic resistance frequencies in Streptococcus pneumonia. Sci Adv. 2020;6:eaaz6137.22.
7) Bakkeren E, et.al. Evolutionary causes and consequences of bacterial antibiotic persistence, Nat Rev Microbiol.2020;18:479-490.
8) Lewnard J A, et.al. Childhood vaccines and antibiotic use in low- and middle-income countries, Nature. 2020;581:94-99.
9) Quinton L J, et.al. Integrative Physiology of Pneumonia. Physiol Rev.2018;98:1417-1464.
10) Qiu J, et.al. Baicalin protects mice from Staphylococcus aureus pneumonia via inhibition of the cytolytic activity of alpha-hemolysin. J Infect Dis.2012; 206;292-301.
11) Chen Z G, et.al. Antiviral effects of Jinxin oral liquid against respiratory syncytial virus infection in the BALB/c mice model.J Ethnopharmacol.2015;162:287-95.
12) Gong L, et.al. Exploration of anti-inflammatory mechanism of forsythiaside A and forsythiaside B in CuSO4-induced inflammation in zebrafish by metabolomic and proteomic analyses. J Neuroinflammation.2020;17:173.

e-ISSN: 2320-3528
p-ISSN: 2347-2286

13) Yang L, et.al.Protective Effect of Phillyrin on Lethal LPS-Induced Neutrophil Inflammation in Zebrafish. Cell Physiol Biochem.2017;43:2074-2087.
14) Zhang H,et.al. Baicalein mediates protection against Staphylococcus aureus-induced pneumonia by inhibiting the coagulase activity of vWbp. Biochem Pharmacol.2020; 178:114024.
15) Zhang B, et.al. Proteogenomic characterization of human colon and rectal cancer. Nature.2014; 513;382-387.
16) Dai J, et.al.Chemoproteomics reveals baicalin activates hepatic CPT1 to ameliorate diet-induced obesity and hepatic steatosis. Proc Natl Acad Sci U S A 2018;115;E5896-E5905.
17) Shen Y, et.al. Loss-of-function mutations in QRICH2 cause male infertility with multiple morphological abnormalities of the sperm flagella. Nat Commun.2019;10:2289.
18) Klein M, et.al. Innate immunity to pneumococcal infection of the central nervous system depends on toll-like receptor (TLR) 2 and TLR4. J Infect Dis.2008;198;1028-1036.
19) Swanson K V, et.al. The NLRP3 inflammasome: molecular activation and regulation to therapeutics.Nat Rev Immunol. 2019;19:477-489.
20) Fang R, et.al. Critical roles of ASC inflammasomes in caspase-1 activation and host 24 innate resistance to Streptococcus pneumoniae infection.J Immunol.2011; 187:4890-4899.
21) Cruz C S D, et.al. Chitinase 3-like-1 promotes Streptococcus pneumoniae killing and augments host tolerance to lung antibacterial responses. Cell Host Microbe.2012; 12:34-46.
22) Hassane M, et.al. Neutrophilic NLRP3 inflammasome-dependent IL-1beta secretion regulates the gammadeltaT17 cell response in respiratory bacterial infections. Mucosal Immunol.2017; 10:1056-1068.
23) Lemon J K, et.al. Sensing of interleukin-1 cytokines during Streptococcus pneumoniae colonization contributes to macrophage recruitment and bacterial clearance. Infect Immun.2015; 83:3204-3212.
24) Lieshout M H P V, et.al. ASC and NLRP3 impair host defense during lethal pneumonia caused by serotype 3 Streptococcus pneumoniae in mice, Eur J Immunol.2018;48: 66-79.
25) McNeela E A, et.al. Pneumolysin activates the NLRP3 inflammasome and promotes proinflammatory cytokines independently of TLR4.PLoS Pathog.2010;6:e1001191.
26) Hoegen T, et.al. The NLRP3 inflammasome contributes to brain injury in pneumococcal meningitis and is activated through ATP-dependent lysosomal cathepsin B release.J Immunol.2011; 187:5440-5451.
27) Hu Y,et.al.Activation of MTOR in pulmonary epithelium promotes LPS-induced acute lung injury. Autophagy. 2016; 12:2286-2299.
28)] Cadwell K. Crosstalk between autophagy and inflammatory signalling pathways: balancing defence and homeostasis. Nat Rev Immunol.2016;16:661-675.
29) Roger J C,et.al. Hypoxia ameliorates intestinal inflammation through NLRP3/mTOR downregulation and autophagy activation. Nat Commun.2017; 8:98.
30) Nakahira K, et.al. Autophagy proteins regulate innate immune responses by inhibiting the release of mitochondrial DNA mediated by the NALP3 inflammasome. Nat Immunol.2011; 12: 222-230.
31) Zhou R, et.al. A role for mitochondria in NLRP3 inflammasome activation. Nature.2011;469;221-225.
32) Shi C S, et.al.Activation of autophagy by inflammatory signals limits IL-1beta production by targeting ubiquitinated inflammasomes for destruction. Nat Immunol.2012;13:255-263.

e-ISSN: 2320-3528
p-ISSN: 2347-2286

33) Wang D, et.al. Not only dopamine D2 receptors involved in Peony-Glycyrrhiza Decoction, an herbal preparation against antipsychotic-associated hyperprolactinemia. Prog Neuropsychopharmacol Biol Psychiatry. 2012;39:332-338.
34) Huang Q, et.al. DiDang Tang Inhibits Endoplasmic Reticulum Stress-Mediated Apoptosis Induced by Oxygen Glucose Deprivation and Intracerebral Hemorrhage Through Blockade of the GRP78-IRE1/PERK Pathways, Front Pharmacol.2018;9:1423.
35) Li T, et.al. Flavonoid profiling of a traditional Chinese medicine formula of Huangqin Tang using high performance liquid chromatography. Acta Pharm Sin B.2016;6: 148-157.
36) Berry A M, et.al. Reduced virulence of a defined pneumolysin-negative mutant of Streptococcus pneumoniae. Inf Imm.1989; 57:2037-2042.
37) Dessing M C, et.al. Toll-like receptor 2 contributes toantibacterial defence against pneumolysin-deficient pneumococci. Cel Microbiol.2008;10; 237-246.
38) Dessing M C, et.al. CD14 Facilitates Invasive Respiratory Tract Infection by Streptococcus pneumoniae. Am.j.respir.crit.care Med.2007; 175:604-611.
39) Nouri-Aria K T, et.al. Grass pollen immunotherapy induces mucosal and peripheral IL-10 responses and blocking IgG activit. J Immunol.2004;172:3252-3259.
40) Renckens R, et.al. Plasminogen activator inhibitor type 1 is protective during severe Gram-negative pneumonia. Blood.2007; 109:1593-1601.
41) Dai J, et.al. Chemoproteomics reveals baicalin activates hepatic CPT1 to ameliorate diet-induced obesity and hepatic steatosis. Proc Natl Acad Sci U S A.2018;115; E5896-E5905.
42) Zahlten J, et.al.TLR9- and Src-dependent expression of Krueppel-like factor 4 controls interleukin-10 expression in pneumonia. Eur Respir J.2013; 41:384-391.
43) Wu S, et.al. Salmonella Interacts With Autophagy to Offense or Defense. Front Microbiol. 2020;11:721.
44) Liu Y, et.al. Ginkgolic acid induces interplay between apoptosis and autophagy regulated by ROS generation in colon cancer.Biochem Biophys Res Commun.2018; 498:246-253.
45) Shi C S, et.al. Activation of autophagy by inflammatory signals limits IL-1β production by targeting ubiquitinated inflammasomes for destruction. Nat Immunol.2012; 13:255-263.
46) Zhou R, et.al. A role for mitochondria in NLRP3 inflammasome activation. Nature.2011; 469: 221-225.
47) Salminen A, et.al. Inflammaging: disturbed interplay between autophagy and inflammasomes. Aging.2012;4:166-175.
48) GBD Lower Respiratory Infections Collaborators. Estimates of the global, regional, and national morbidity, mortality, and aetiologies of lower respiratory infections in 195 countries, 1990-2016: a systematic analysis for the Global Burden of Disease Study 2016. Lancet Infect Dis.2018;18:1191-1210.
49) Quinton L J, et.al. Integrative Physiology of Pneumonia. Phy Rev.2018;98:1417-1464.
50) Kadri S S, et.al. Efforts to Curb Antibiotic Resistance — Are We Saving Lives? N Eng J Med.2020; 383:806-808.
51) Wang D, et.al. Hormesis as a mechanistic approach to understanding herbal treatments in traditional Chinese medicine. Pharmacol Therap.2018;184:42-50.

e-ISSN: 2320-3528
p-ISSN: 2347-2286

52) Lai L, et.al. Chinese Herbal Medicine for Oligomenorrhoea and Amenorrhoea in Polycystic Ovary Syndrome: A Systematic Review and Meta-Analysis. J Alt Compl Med..2014;20:A129.

53) Qui J, et.al. Baicalin protects mice from Staphylococcus aureus pneumonia via inhibition of the cytolytic activity of α-hemolysin. J Infect Dis. 2012;206: 292-301.

54) Peng L Y, et.al. Baicalin alleviated APEC-induced acute lung injury in chicken by inhibiting NF-κB pathway activation. Int immunopharmacol.2019;72:467-472.

55) Chen Z G, et.al. Antiviral effects of Jinxin oral liquid against respiratory syncytial virus infection in the BALB/c mice model. J Ethnopharmacol.2015;162:287-295.

56) Zhang H, et.al.Baicalein mediates protection against Staphylococcus aureus-induced pneumonia by inhibiting the coagulase activity of vWbp. Biochem Pharmacol.2020;178:114024.

57) Zhong W T, et.al. Phillyrin attenuates LPS-induced pulmonary inflammation via suppression of MAPK and NF-κB activation in acute lung injury mice. Fitoterapia.2013;90:132-139.

58) Ma G Z, et.al. Baicalein Inhibits DMBA/TPA-Induced Skin Tumorigenesis in Mice by Modulating Proliferation, Apoptosis, and 30 Inflammation. Inflammation.2013;36:457-467.

59) Gong L, et.al.Exploration of anti-inflammatory mechanism of forsythiaside A and forsythiaside B in CuSO4-induced inflammation in zebrafish by metabolomic and proteomic analyses. J Neuroinflammation.2020;17:173.

60) Hu Y, et.al. Activation of MTOR in pulmonary epithelium promotes LPS-induced acute lung injury. Autophagy.2016;12:2286-2299.

61) Kim J Y, et.al. Streptococcus pneumoniae induces pyroptosis through the regulation of autophagy in murine microglia. Oncotarget.2015;6:44161-44178.

62) Malley R, et.al. Recognition of pneumolysin by Toll-like receptor 4 confers resistance to pneumococcal infection, Proc Natl Acad Sci U S A . 2003;100:1966-1971.

63) Koppe U, et.al. Recognition of Streptococcus pneumoniae by the innate immune system. Cell Microbiol.2012;14:460-466.